Journal of Engineering Mathematics **40:** 315–332, 2001.

Stress analysis of axisymmetric shear deformable cross-ply laminated circular cylindrical shells

A. M. ZENKOUR
Department of Mathematics, Faculty of Education, Tanta University, Kafr El-Sheikh 33516, Egypt
(e-mail: Zenkour@edu-kaf.edu.eg)

Received 1 November 1999; accepted in revised form 2 November 2000

Abstract. A generalized mixed theory for bending analysis of axisymmetric shear deformable laminated circular cylindrical shells is presented. The classical, first-order and higher-order shell theories have been used in the analysis. The Maupertuis–Lagrange (M–L) mixed variational formula is utilized to formulate the governing equations of circular cylindrical shells laminated by orthotropic layers. Analytical solutions are presented for symmetric and antisymmetric laminated circular cylindrical shells under sinusoidal loads and subjected to arbitrary boundary conditions. Numerical results of the higher-order theory for deflections and stresses of cross-ply laminated circular cylindrical shells are compared with those obtained by means of the classical and first-order shell theories. The effects, due to shear deformation, lamination schemes, loadings ratio, boundary conditions and orthotropy ratio on the deflections and stresses are investigated.

Key words: bending response, closed circular cylindrical shells, variational approach.

1. Introduction

Shell structures find application in many fields of engineering, notably civil, mechanical and aeronautical disciplines. The generally high strength-to-weight ratio of the shell form, combined with its inherent stiffness, has formed the basis of modern applications of shell structures. For example, in the marine industry, composite shell structures are considered for submersible hulls or for the support columns in offshore platforms. Furthermore, composite shell structural configurations of moderate thickness can be potentially used for components in the automobile industry and in space vehicles as a primary load-carrying structure. Of all existing shell models, the circular cylindrical shell is perhaps the most widely studied. It has applications in chimney design, pipe flow, and aircraft fuselages, to name a few. Cylindrical shells are also widely used as tanks, boilers, gas and water conduits, cisterns, etc.

A shell may be defined as a relatively thin structural element, in which the material of the element is bound between two curved surfaces that are a relatively small distance apart. The behavior of a shell is usually modeled on the basis of its middle surface (alternatively referred to as mid-surface), which is the locus of interior points equidistant from two bounding surfaces of the shell [1, pp. 1–22].

A number of theories for laminated composite shells exists in the literature. Shells are often modeled using the classical (*i.e.*, Love–Kirchhoff first-approximation) shell theory [2–6], which does not account for transverse shear strains. One of the important characteristics of most of the present-day advanced composites is the high ratio of extensional-to-shear modulus. This may render the classical theories inadequate for the analysis of moderately thick composite shells. The higher-order shear deformation theories could potentially produce

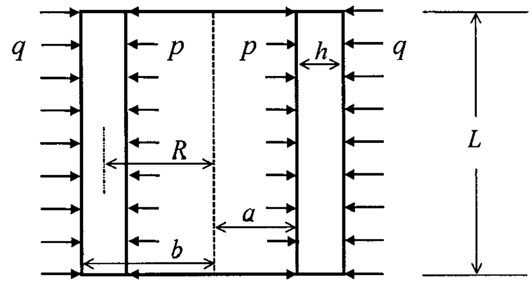

Figure 1. Closed circular cylindrical shell under internal and external loads.

much more accurate results. Several refined shell theories and models have been developed in the last three decades [6–21].

The governing equations of higher-order, often not exceeding third-order, shell theories are very complicated. They are simplified if their deformations are axisymmetric, *i.e.* derivatives with respect to the circumferential coordinate are equal to zero. Recently, Zenkour [22] has developed a higher-order shear deformable shell theory for the vibration analysis of axisymmetric deformable layered orthotropic circular cylindrical shells. The governing equations were obtained using the M–L mixed variational formula [23]. Another mixed variational formula based upon Hamilton's principle has been presented by Zenkour [24] for laminated structures (see also [25–28]). This mixed variational formula is an extension to earlier work [29] for homogeneous structures (see also [30]).

The present work uses a mixed generalization of the higher-order shell theory of Zenkour [22] to study the bending of cross-ply laminated closed circular cylindrical shells. Governing equations are obtained using the M–L mixed variational formula. Once again, the M–L mixed variational formula is used to find the analytical solutions of the theory for a variety of boundary conditions and lamination schemes. Numerical results for deflections and stresses obtained using the classical, first-order and higher-order shell theories are compared.

2. Derivation of various shell theories

Consider a fiber-reinforced laminated composite circular cylindrical shell of finite length L and total wall thickness h (see Figure 1). Let the shell undergo bending due to internal and external loads $p(z)$ and $q(z)$, respectively. The closed circular cylindrical shell under consideration is composed of a finite number, N, of uniform-thickness orthotropic layers.

In the case of linear axisymmetric deformation, the points of the shell displace in the radial and axial directions only and these displacements are independent of the angle θ. The most commonly used shell theory is the classical theory, which is based on the displacement field

$$u_r(r,z) = u(z), \qquad u_z(r,z) = w(z) - \xi\frac{\mathrm{d}u}{\mathrm{d}z}, \tag{2.1}$$

where (u_r, u_z) are the displacements along the (ξ, z) coordinates; (u, w) are the radial and axial components of the displacement of a point on the mid-surface of the shell. It is to be noted that the thickness coordinate ξ is introduced here, instead of the radial coordinate r, such that (A notation of all symbols is given in Appendix A):

$$r = R\left(1+\frac{\xi}{R}\right), \qquad \xi_0 \le \xi \le \xi_N, \qquad R = \frac{a+b}{2}. \tag{2.2}$$

The displacement field (2.1) implies that straight lines normal to the mid-surface before deformation remain straight and normal to the mid-surface after deformation. It is clear that, for the classical theory, all strains except ε_{zz} are zero. The first-order shear deformation shell theory is based on the displacement field

$$u_r(r,z) = u(z), \qquad u_z(r,z) = w + \xi\varphi(z), \tag{2.3}$$

where φ is the rotation of the normal to the mid-surface at $\xi = 0$. The following displacement field of the higher-order shear deformation shell theory can be found in Zenkour [22]:

$$u_r(r,z) = u(z), \quad u_z(r,z) = w(z) + \xi\left[\varphi(z) - \frac{1}{3}\left(\frac{\xi}{h/2}\right)^2\left(\frac{\mathrm{d}u}{\mathrm{d}z} + \varphi(z)\right)\right]. \tag{2.4}$$

All technical shell theories up to and including higher-orders, in the case of axisymmetric shear deformation cylindrical shells, can be derived from the displacement field

$$u_r(r,z) = u(z), \quad u_z(r,z) = w(z) + \xi\left[\alpha\frac{\mathrm{d}u}{\mathrm{d}z} + \beta\varphi(z) + \gamma\xi^2\left(\frac{\mathrm{d}u}{\mathrm{d}z} + \varphi(z)\right)\right]. \tag{2.5}$$

The above displacement field contains the displacement field of the classical shell theory, the first-order shear deformation shell theory and the higher-order shear deformation shell theory. We have

(i) Classical Shell Theory (CST): $\alpha = -1, \beta = \gamma = 0$;

(ii) First-order Shell Theory (FST): $\alpha = 0, \beta = 1; \gamma = 0$;

(iii) Higher-order Shell Theory (HST): $\alpha = 0, \beta = 1, \gamma = -4/(3h^2)$.

The classical shell theory can also be obtained from the first-order shell theory by setting $\varphi = -\mathrm{d}u/\mathrm{d}z$.

Substituting Equation (2.5) in the strain-displacement relations referred to the cylindrical coordinate system, taking into account that derivatives with respect to the circumferential coordinate are equal to zero, we obtain

$$\begin{aligned}
&\varepsilon_1 = \varepsilon_{rr} = \frac{\partial u_r}{\partial r} = 0, \quad \varepsilon_2 = \varepsilon_{\theta\theta} = \frac{u_r}{r} = \frac{u}{R}\left(1 + \frac{\xi}{R}\right)^{-1},\\
&\varepsilon_3 = \varepsilon_{zz} = \frac{\partial u_z}{\partial z} = \frac{\mathrm{d}w}{\mathrm{d}z} + \xi\left[\alpha\frac{\mathrm{d}^2u}{\mathrm{d}z^2} + \beta\frac{\mathrm{d}\varphi}{\mathrm{d}z} + \gamma\xi^2\left(\frac{\mathrm{d}^2u}{\mathrm{d}z^2} + \frac{\mathrm{d}\varphi}{\mathrm{d}z}\right)\right], \quad \varepsilon_4 = 2\varepsilon_{\theta z} = 0,\\
&\varepsilon_5 = 2\varepsilon_{rz} = \frac{\partial u_r}{\partial z} + \frac{\partial u_z}{\partial r} = (1+\alpha)\frac{\mathrm{d}u}{\mathrm{d}z} + \beta\varphi + 3\gamma\xi^2\left(\frac{\mathrm{d}u}{\mathrm{d}z} + \varphi\right), \quad \varepsilon_6 = 2\varepsilon_{r\theta} = 0.
\end{aligned} \tag{2.6}$$

3. Mixed variational formulation

The first-order shell theory includes a constant state of transverse shear strain with respect to the thickness coordinate. In fact, it requires a shear correction factor, which depends not only on the material and geometric parameters, but also on the loading and boundary conditions. In addition, the higher-order shell theory involves additional higher-order stress resultants and material stiffness coefficients compared to the first-order shell theory. The utilization of the mixed variational principles allows one to deduce rational deformation theories for laminated structures without introducing shear correction factors for the first-order theory or using additional higher-order stress resultants for the higher-order theory. As is well known, in these principles both the displacements u_i and stresses σ_{ij} are considered to be arbitrary. The mixed variational principles can be applied to the fundamental mixed problem of the theory of elasticity, in which the surface forces F_i^* are prescribed over a part S_σ of the total surface of the body and the displacements u_i^* are prescribed over the remaining surface S_u.

The Maupertuis–Lagrange (M–L) principle states that the integral

$$W = \int_{t_1}^{t_2} 2T \,\mathrm{d}t \tag{3.1}$$

has a stationary value for any part of an actual trajectory, provided that the energy of the system is conserved;

$$T + \Pi = \text{ constant } = H, \tag{3.2}$$

and the total variation of displacements Δu_i satisfies

$$\Delta u_i|_{t_1} = \Delta u_i|_{t_2} = 0. \tag{3.3}$$

The kinetic energy T and the total potential energy Π are given, respectively, by:

$$T = \frac{1}{2} \iiint_V \rho \dot{u}_i \dot{u}_i \,\mathrm{d}V, \tag{3.4}$$

$$\Pi = \iiint_V \left[\sigma_{ij}\varepsilon_{ij} - R(\sigma_{ij}) - F_i u_i\right] \mathrm{d}V - \iint_{S_\sigma} F_i^* u_i \,\mathrm{d}S, \tag{3.5}$$

where $\rho = \rho^{(k)}$ is the material density of layer k, F_i are the body forces and $R(\sigma_{ij})$ is called the additional work (complementary energy density). The expression for $R(\sigma_{ij})$ of an orthotropic structure takes the form [31, pp. 24–37]:

$$\begin{aligned} R(\sigma_{ij}) = {} & \tfrac{1}{2}(a_{11}\sigma_1^2 + a_{22}\sigma_2^2 + a_{33}\sigma_3^2 + a_{44}\sigma_4^2 + a_{55}\sigma_5^2 + a_{66}\sigma_6^2) \\ & + a_{12}\sigma_1\sigma_2 + a_{23}\sigma_2\sigma_3 + a_{31}\sigma_3\sigma_1, \end{aligned} \tag{3.6}$$

where $a_{ij} = a_{ij}^{(k)}$ are the compliance constants, which depend on the material properties and orientation of the kth layer. Here, we have written $\sigma_1, \sigma_2, \sigma_3, \sigma_4, \sigma_5, \sigma_6$ in place of the conventional $\sigma_{rr}, \sigma_{\theta\theta}, \sigma_{zz}, \sigma_{\theta z}, \sigma_{rz}$ and $\sigma_{r\theta}$.

Now, the problem is to determine the extremum of the functional (3.1), subject to condition (3.2). We introduce the Lagrange's multipliers λ and λ_i to obtain the unconditional functional

$$J = W + \int_{t_1}^{t_2} \left[\lambda(T + \Pi - H) + \iint_{S_u} \lambda_i \left(u_i - u_i^*\right) \mathrm{d}S\right] \mathrm{d}t. \tag{3.7}$$

The extremum condition of the above functional takes place when (for more details, we refer to Zenkour [23])

$$\lambda = -1 \qquad \text{and} \qquad \lambda_i = n_j \sigma_{ij}, \tag{3.8}$$

where n_j are the components of the unit vector along the outward normal to the surface. Therefore, we get the M–L mixed variational formula (3.7) in the following final form [22, 23]:

$$J = \int_{t_1}^{t_2} \left[T - \Pi + H + \iint_{S_u} n_j \sigma_{ij} \left(u_i - u_i^* \right) \mathrm{d}S \right] \mathrm{d}t. \tag{3.9}$$

For this problem, the stress components are given by the author's previous paper [22] as follows:

$$\begin{aligned}
\sigma_1 &= -\frac{p}{4}\left[2 - 3\left(\frac{\xi}{h/2}\right) + \left(\frac{\xi}{h/2}\right)^3\right] - \frac{q}{4}\left[2 + 3\left(\frac{\xi}{h/2}\right) - \left(\frac{\xi}{h/2}\right)^3\right],\\
\sigma_2 &= \frac{N_2}{h} + \frac{12M_2}{h^3}\xi, \quad \sigma_3 = \left[\frac{N_3}{h} + \frac{12M_3}{h^3}\xi\right]\left(1 + \frac{\xi}{R}\right)^{-1},\\
\sigma_5 &= \frac{3Q}{2h}\left[1 - \left(\frac{\xi}{h/2}\right)^2\right]\left(1 + \frac{\xi}{R}\right)^{-1}, \quad \sigma_4 = \sigma_6 = 0,
\end{aligned} \tag{3.10}$$

where (N_2, N_3, Q) are the in-plane tangential, axial and shearing forces, respectively, and (M_2, M_3) are bending moments

$$\begin{aligned}
\{N_2, N_3, Q\} &= \int_{-h/2}^{+h/2} \left\{\sigma_2, \sigma_3\left(1 + \frac{\xi}{R}\right), \sigma_5\left(1 + \frac{\xi}{R}\right)\right\} \mathrm{d}\xi,\\
\{M_2, M_3\} &= \int_{-h/2}^{+h/2} \xi \left\{\sigma_2, \sigma_3\left(1 + \frac{\xi}{R}\right)\right\} \mathrm{d}\xi.
\end{aligned} \tag{3.11}$$

It is clear that the transverse shear stress σ_5 is continuous through the thickness and vanishes on the bounding surface of the shell. Also, the radial stress σ_1 has extremum values on the inner and outer cylindrical surfaces of the shell and satisfies the conditions

$$\sigma_1 = -p(z) \quad \text{at} \quad \xi = \xi_0 \quad \text{and} \quad \sigma_1 = -q(z) \quad \text{at} \quad \xi = \xi_N. \tag{3.12}$$

In addition, this radial stress is the same for all shell theories and various lamination schemes and boundary conditions.

4. Governing equations

The static model of the M–L mixed variational formula (3.9) is used to derive the equilibrium and constitutive equations of the axisymmetric shear deformable laminated circular cylindrical shell. This formula will be applied to the present problem in the absence of the body forces and prescribed displacements. Substituting Equations (2.5), (2.6), and (3.10) in the functional Equation (3.9), we can easily get the total variation of this functional. In this case, the extremum condition gives the following system of equilibrium equations:

$$\delta u : \frac{\mathrm{d}Q}{\mathrm{d}z} + \left(\alpha + \frac{3h^2}{20}\gamma\right)\frac{\mathrm{d}\hat{Q}}{\mathrm{d}z} - \frac{N_2}{R} - \frac{h}{2R}(p + q) + (p - q) = 0, \tag{4.1}$$

$$\delta w : \frac{\mathrm{d}N_3}{\mathrm{d}z} = 0, \qquad \delta\varphi : -\left(\beta + \frac{3h^2}{20}\gamma\right)\hat{Q} = 0, \qquad (4.2)\ (4.3)$$

where

$$\hat{Q} = Q - \frac{\mathrm{d}M_3}{\mathrm{d}z}. \tag{4.4}$$

Clearly, the above equilibrium equations do not contain any correction factors for FST and have the same stress resultants for HST and FST. The extremum condition gives also the following constitutive equations:

$$\begin{Bmatrix} N_2 \\ N_3 \\ Q \\ M_2 \\ M_3 \end{Bmatrix} = \begin{bmatrix} A_{22} & A_{23} & 0 & B_{22} & B_{23} \\ & A_{33} & 0 & B_{23} & B_{33} \\ & & A_{55} & 0 & 0 \\ & & & D_{22} & D_{23} \\ \text{symm.} & & & & D_{33} \end{bmatrix}^{-1} \begin{Bmatrix} \dfrac{u}{R} + f_2 \\ \dfrac{\mathrm{d}w}{\mathrm{d}z} + f_3 \\ \left(1 + \alpha + \dfrac{3h^2}{20}\gamma\right)\dfrac{\mathrm{d}u}{\mathrm{d}z} + \left(\beta + \dfrac{3h^2}{20}\gamma\right)\varphi \\ g_2 \\ \left(\alpha + \dfrac{3h^2}{20}\gamma\right)\dfrac{\mathrm{d}^2u}{\mathrm{d}z^2} + \left(\beta + \dfrac{3h^2}{20}\gamma\right)\dfrac{\mathrm{d}\varphi}{\mathrm{d}z} + g_3 \end{Bmatrix}. \tag{4.5}$$

The following definitions are used in the above equation:

$$\{A_{ij}, B_{ij}, D_{ij}\} = \sum_{k=1}^{N} \int_{\xi_{k-1}}^{\xi_k} a_{ij}^{(k)} \left\{\frac{1}{h^2}, \frac{12}{h^4}\xi, \frac{144}{h^6}\xi^2\right\} \left(1 + \frac{\xi}{R}\right)^{\eta} \mathrm{d}\xi, \tag{4.6}$$

$$A_{55} = \frac{9}{4h^2} \sum_{k=1}^{N} \int_{\xi_{k-1}}^{\xi_k} a_{55}^{(k)} \left[1 - \left(\frac{\xi}{h/2}\right)^2\right]^2 \left(1 + \frac{\xi}{R}\right)^{-1} \mathrm{d}\xi, \tag{4.7}$$

$$f_j = A_{1j}^{(-1)} p + A_{1j}^{(+1)} q, \quad g_j = B_{1j}^{(-1)} p + B_{1j}^{(+1)} q, \tag{4.8}$$

and

$$\left\{A_{1j}^{(\lambda)}, B_{1j}^{(\lambda)}\right\} = \sum_{k=1}^{N} \int_{\xi_{k-1}}^{\xi_k} \frac{a_{1j}^{(k)}}{4} \left\{\frac{1}{h}, \frac{12}{h^3}\xi\right\} \left[2 + 3\lambda\left(\frac{\xi}{h/2}\right) - \lambda\left(\frac{\xi}{h/2}\right)^3\right] \left(1 + \frac{\xi}{R}\right)^{3-j} \mathrm{d}\xi, \tag{4.9}$$

where

$$i, j = 2, 3; \quad \lambda = \pm 1; \quad \eta = \begin{cases} 1 \text{ if } i = j = 2, \\ 0 \text{ if } i \neq j, \\ -1 \text{ if } i = j = 3. \end{cases} \tag{4.10}$$

In addition to the above equilibrium and constitutive equations, the M–L mixed variational formula indicates that the essential and the natural boundary conditions of the problem are given in Table 1.

5. Analytical solutions

The solution procedure used in Zenkour [22] will be extended here in order to analyze the bending of cross-ply laminated cylindrical shells. The following three sets of boundary conditions for simply supported (SS), clamped-simply supported (CS) and clamped (CC) at the edges $z = 0, L$ for the three theories are used:

Table 1. Boundary conditions

Essential	Natural
u	$Q + \left(\alpha + \frac{3h^2}{20}\gamma\right)\hat{Q}$
w	N_3
$\frac{\mathrm{d}u}{\mathrm{d}z}$	$\left(\alpha + \frac{3h^2}{20}\gamma\right) M_3$
φ	$\left(\beta + \frac{3h^2}{20}\gamma\right) M_3$

$$\begin{aligned}
\text{HST}: \quad & SS: u = N_3 = M_3 = 0 \quad \text{at} \quad z = 0, L;\\
& CS: u = w = \frac{\mathrm{d}u}{\mathrm{d}z} = \varphi = 0 \quad \text{at} \quad z = 0; u = N_3 = M_3 = 0 \quad \text{at} \quad z = L;\\
& CC: u = w = \frac{\mathrm{d}u}{\mathrm{d}z} = \varphi = 0 \quad \text{at} \quad z = 0, L.
\end{aligned} \tag{5.1}$$

$$\begin{aligned}
\text{FST}: \quad & SS: u = N_3 = M_3 = 0 \quad \text{at} \quad z = 0, L;\\
& CS: u = w = \varphi = 0 \quad \text{at} \quad z = 0; \quad u = N_3 = M_3 = 0 \quad \text{at} \quad z = L;\\
& CC: u = w = \varphi = 0 \quad \text{at} \quad z = 0, L.
\end{aligned} \tag{5.2}$$

$$\begin{aligned}
\text{CST}: \quad & SS: u = N_3 = M_3 = 0 \quad \text{at} \quad z = 0, L;\\
& CS: u = w = \frac{\mathrm{d}u}{\mathrm{d}z} = 0 \quad \text{at} \quad z = 0; u = N_3 = M_3 = 0 \quad \text{at} \quad z = L;\\
& CC: u = w = \frac{\mathrm{d}u}{\mathrm{d}z} = 0 \quad \text{at} \quad z = 0, L.
\end{aligned} \tag{5.3}$$

The following representation for the displacement quantities is appropriate in the analysis of the bending problem:

$$\left\{ \begin{array}{c} u \\ w \\ \varphi \end{array} \right\} = \left\{ \begin{array}{ll} U_m & \chi(\mu_m z) \\ W_m & \chi'(\mu_m z) \\ \Phi_m & \chi'(\mu_m z) \end{array} \right\}. \tag{5.4}$$

The function $\chi(\mu_m z)$ can be constructed for any arbitrary combination of edge conditions. The different forms of $\chi(\mu_m z)$ and the corresponding values of μ_m are defined in [22] (see also [32, pp. 339–343]). The representation given for u, w, and φ in Equation (5.4) is valid for all three theories: HST, FST and CST. In addition, the following sinusoidally distributed loads are used

$$\{p(z), q(z)\} = \{p_0, q_0\} \sin \frac{\pi z}{L}, \tag{5.5}$$

where p_0 and q_0 represent the intensity of the internal and external loads at the center of the shell, respectively.

Substitution of Equations (5.4) and (5.5), with the aid of Equation (4.5), in the static form of the total variation of the functional Equation (3.9) yields a set of three (two) algebraic equations in terms of the unknown amplitudes U_m, W_m and Φ_m for HST and FST (U_m and W_m for CST). These equations can be expressed in matrix form as

$$[C]\{\Delta\} = \{F\}, \tag{5.6}$$

where $\{\Delta\}$ and $\{F\}$ denote the columns

$$\left.\begin{aligned} \{\Delta\}^{\mathrm{T}} &= \{U_m, W_m, \Phi_m\}, \\ \{F\}^{\mathrm{T}} &= \left\{F_1^m, F_2^m, F_3^m\right\}, \end{aligned}\right\} \quad \text{for HST and FST,} \tag{5.7}$$

or

$$\left.\begin{aligned} \{\Delta\}^{\mathrm{T}} &= \{U_m, W_m\}, \\ \{F\}^{\mathrm{T}} &= \left\{F_1^m, F_2^m\right\}, \end{aligned}\right\} \quad \text{for CST.} \tag{5.8}$$

For all theories and various boundary conditions, the elements of matrix $[C]$ and force vector $\{F\}$ are defined in Appendix B.

Thus, for a given $\chi(\mu_m z)$, $F_i^m(m = 1)$, and cross-ply construction, one needs to solve the 3×3 (2×2 for CST) matrix Equation (5.6) for the vector of amplitudes of the generalized displacements.

6. Numerical results

The numerical applications are done for symmetric and antisymmetric cross-ply circular cylindrical shells. It is assumed that the thickness and the material properties for all laminae are the same. The results were produced for a typical graphite/epoxy material with moduli of 10^6 psi and Poisson's ratios listed below, where subscript 1 is the radial r-direction, 2 the circumferential θ-direction, and 3 the axial z-direction: $E_1 = 19{\cdot}2$, $E_2 = 1{\cdot}456$, $E_3 = 1{\cdot}56$, $G_{12} = G_{13} = 0{\cdot}82$, $G_{23} = 0{\cdot}523$, $\nu_{12} = \nu_{31} = 0{\cdot}24$, and $\nu_{32} = 0{\cdot}49$. For the present problem, the compliances a_{ij} may be expressed in terms of the engineering orthotropic characteristics as:

$$a_{22} = \frac{1}{E_2}, \quad a_{33} = \frac{1}{E_3}, \quad a_{12} = -\frac{\nu_{12}}{E_1}, \quad a_{13} = -\frac{\nu_{31}}{E_3}, \quad a_{23} = -\frac{\nu_{32}}{E_3}, \quad a_{55} = \frac{1}{G_{13}}.$$

We will assume in all the analyzed cases (unless otherwise stated) that $q_0 = 0$, $L/R = 1$ and $R/h = 10$.

The following nondimensional response characteristics

$$\overline{u}\left[= u\left(\xi, \frac{L}{2}\right)\frac{100h^3}{a_{22}p_0R^4}\right]; \quad \overline{\sigma}_2\left[= \sigma_2\left(\frac{h}{2}, \frac{L}{2}\right)\frac{10h^2}{p_0R^2}\right]; \quad \overline{\sigma}_3\left[= \sigma_3\left(\frac{h}{2}, \frac{L}{2}\right)\frac{10h^2}{p_0R^2}\right],$$

determined as per the higher-order shell theory (HST), are compared with those obtained by the classical (CST) and first-order (FST) shell theories. The numerical results for the lamination schemes (0°/90°/...) are displayed in Tables 2–5 as well as in Figures 2–9.

Table 2. The effect of radius-to-thickness ratio on the center deflection ($\overline{u}$) of cross-ply circular cylindrical shells for various boundary conditions

R/h	Theory	0°/90°			0°/90°/ 0°			0°/90°/... 10 layers		
		SS	CS	CC	SS	CS	CC	SS	CS	CC
2	HST	6·8442	2·9693	1·7662	6·9849	3·0058	1·7824	7·1768	3·0698	1·8091
	FST	6·9183	2·9875	1·7703	7·0548	3·0226	1·7862	7·2327	3·0835	1·8122
	CST	4·9750	1·5361	0·5928	5·0473	1·5378	0·5893	5·2718	1·6145	0·6204
4	HST	3·3839	1·4545	0·7825	3·4439	1·4663	0·7845	3·4691	1·4833	0·7944
	FST	3·3963	1·4591	0·7843	3·4558	1·4705	0·7862	3·4787	1·4868	0·7958
	CST	3·2236	1·2562	0·5645	3·2764	1·2601	0·5604	3·3082	1·2835	0·5748
10	HST	0·8315	0·4284	0·2616	0·8472	0·4345	0·2638	0·8411	0·4329	0·2640
	FST	0·8321	0·4287	0·2618	0·8477	0·4348	0·2640	0·8415	0·4331	0·2641
	CST	0·8302	0·4249	0·2546	0·8459	0·4309	0·2564	0·8397	0·4295	0·2570
20	HST	0·2290	0·1262	0·0849	0·2329	0·1282	0·0860	0·2304	0·1270	0·0854
	FST	0·2290	0·1262	0·0849	0·2329	0·1282	0·0860	0·2305	0·1270	0·0854
	CST	0·2290	0·1261	0·0847	0·2329	0·1281	0·0858	0·2304	0·1269	0·0852

Table 3. The effect of radius-to-thickness ratio on the circumferential stress ($\overline{\sigma}_2$) of cross-ply circular cylindrical shells for various boundary conditions

R/h	Theory	0°/90°			0°/90°/ 0°			0°/90°/... 10 layers		
		SS	CS	CC	SS	CS	CC	SS	CS	CC
2	HST	2·3918	1·1192	0·6563	2·3245	1·0938	0·6434	2·4828	1·1833	0·6999
	FST	2·4342	1·1365	0·6648	2·3625	1·1092	0·6510	2·5137	1·1959	0·7061
	CST	2·3399	0·9969	0·5131	2·2776	0·9789	0·5090	2·4341	1·0668	0·5630
4	HST	2·1990	1·1271	0·6737	2·1146	1·0814	0·6445	2·1793	1·1243	0·6737
	FST	2·2088	1·1319	0·6763	2·1234	1·0856	0·6468	2·1865	1·1278	0·6757
	CST	2·2256	1·1176	0·6357	2·1420	1·0729	0·6085	0·2063	1·1168	0·6386
10	HST	1·1217	0·6777	0·4759	1·0706	0·6488	0·4553	1·0861	0·6600	0·4649
	FST	1·1225	0·6781	0·4762	1·0713	0·6493	0·4556	1·0866	0·6603	0·4651
	CST	1·1261	0·6820	0·4792	1·0750	0·6533	0·4587	1·0902	0·6643	0·4683
20	HST	0·5635	0·3511	0·2639	0·5341	0·3346	0·2521	0·5407	0·3387	0·2554
	FST	0·5636	0·3512	0·2639	0·5342	0·3347	0·2522	0·5407	0·3387	0·2554
	CST	0·5639	0·3517	0·2647	0·5345	0·3352	0·2530	0·5411	0·3393	0·2562

To assess the importance of shear deformation, the numerical results obtained by all theories have been compared for various boundary conditions and lamination schemes in Tables 2–5. Center deflection, circumferential stress and axial stress of two, three and ten-layer cross-ply cylindrical shells are presented, respectively, in Tables 2–4 as functions of radius-to-thickness ratio (R/h). Table 5 emphasizes the effect of the intensity of external-to-internal loads ratio (q_0/p_0) on the deflection ($\overline{u}$) and stresses ($\overline{\sigma}_2, \overline{\sigma}_3$) for a four-layer symmetric cross-ply circular cylindrical shell.

In Figures 2–8, only the higher-order shell theory is used. Figures 2–4 display, respectively, the variation of $\overline{u}, \overline{\sigma}_2$ and $\overline{\sigma}_3$ *vs.* R/h for a (0°/90°/90°/0°) circular cylindrical shell with dif-

Table 4. The effect of radius-to-thickness ratio on the axial stress ($\overline{\sigma}_3$) of cross-ply circular cylindrical shells for various boundary conditions

R/h	Theory	0°/90°			0°/90°/ 0°			0°/90°/... 10 layers		
		SS	CS	CC	SS	CS	CC	SS	CS	CC
2	HST	2·3430	1·2239	0·7313	2·3908	1·2435	0·7410	2·3757	1·2189	0·7192
	FST	2·3960	1·2492	0·7452	2·4413	1·2674	0·7541	2·4151	1·2377	0·7295
	CST	2·8102	1·4304	0·8206	2·8701	1·4524	0·8303	2·8376	1·4226	0·8063
4	HST	1·7590	1·1270	0·7446	1·7932	1·1465	0·7538	1·7496	1·1243	0·7422
	FST	1·7685	1·1328	0·7483	1·8022	1·1520	0·7573	1·7567	1·1286	0·7450
	CST	1·9281	1·2545	0·8315	1·9697	1·2781	0·8422	1·9170	1·2517	0·8291
10	HST	0·5280	0·4753	0·4159	0·5266	0·4838	0·4245	0·5089	0·4691	0·4139
	FST	0·5285	0·4757	0·4162	0·5270	0·4841	0·4248	0·5092	0·4694	0·4142
	CST	0·5397	0·4913	0·4371	0·5386	0·5006	0·4468	0·5201	0·4850	0·4351
20	HST	0·1584	0·1702	0·1708	0·1507	0·1706	0·1738	0·1466	0·1656	0·1688
	FST	0·1585	0·1702	0·1709	0·1507	0·1706	0·1738	0·1466	0·1656	0·1688
	CST	0·1594	0·1717	0·1734	0·1516	0·1721	0·1765	0·1474	0·1670	0·1714

Table 5. The effect of q_0/p_0 ratio on $\overline{u}$, $\overline{\sigma}_2$ and $\overline{\sigma}_3$ of a (0°/90°/90°/0°) circular cylindrical shell for various boundary conditions

q_0/p_0	Theory	$\overline{u}$			$\overline{\sigma}_2$			$\overline{\sigma}_3$		
		SS	CS	CC	SS	CS	CC	SS	CS	CC
0·2	HST	0·6571	0·3380	0·2057	0·8346	0·5049	0·3546	0·4055	0·3719	0·3273
	FST	0·6575	0·3382	0·2058	0·8352	0·5053	0·3548	0·4058	0·3722	0·3275
	CST	0·6561	0·3352	0·2001	0·8380	0·5084	0·3573	0·4147	0·3352	0·3445
0·5	HST	0·3818	0·1974	0·1205	0·4804	0·2885	0·2023	0·2363	0·2130	0·1874
	FST	0·3820	0·1976	0·1205	0·4808	0·2887	0·2025	0·2365	0·2131	0·1876
	CST	0·3812	0·1958	0·1171	0·4824	0·2905	0·2039	0·2416	0·2205	0·1975
0·7	HST	0·1982	0·1037	0·0636	0·2443	0·1442	0·1008	0·1234	0·1070	0·0942
	FST	0·1983	0·1038	0·0637	0·2445	0·1444	0·1009	0·1235	0·1070	0·0943
	CST	0·1979	0·1029	0·0619	0·2454	0·1453	0·1016	0·1262	0·1110	0·0995
1·0	HST	−0·0772	−0·0369	−0·0217	−0·1099	−0·0722	−0·0515	−0·0458	−0·0520	−0·0456
	FST	−0·0772	−0·0369	−0·0217	−0·1099	−0·0722	−0·0515	−0·0458	−0·0520	−0·0457
	CST	−0·0770	−0·0366	−0·0211	−0·1102	−0·0725	−0·0517	−0·0468	−0·0534	−0·0474

ferent values of q_0/p_0 ratio. Also, Figures 5–7 display, respectively, the variation of $\overline{u}$, $\overline{\sigma}_2$ and $\overline{\sigma}_3$ *vs.* L/R for a (0°/90°/0°/90°) circular cylindrical shell. Figure 8 displays the variation of $\overline{u}$ *vs.* the orthotropy ratio (a_{33}/a_{22}) for a (0°/90°/0°) circular cylindrical shell. Finally, Figure 9 displays the plots of $\overline{\sigma}_1\left[= \sigma_1(\xi, L/2)/p_0\right]$ through the thickness of the shell for different values of q_0/p_0 ratio.

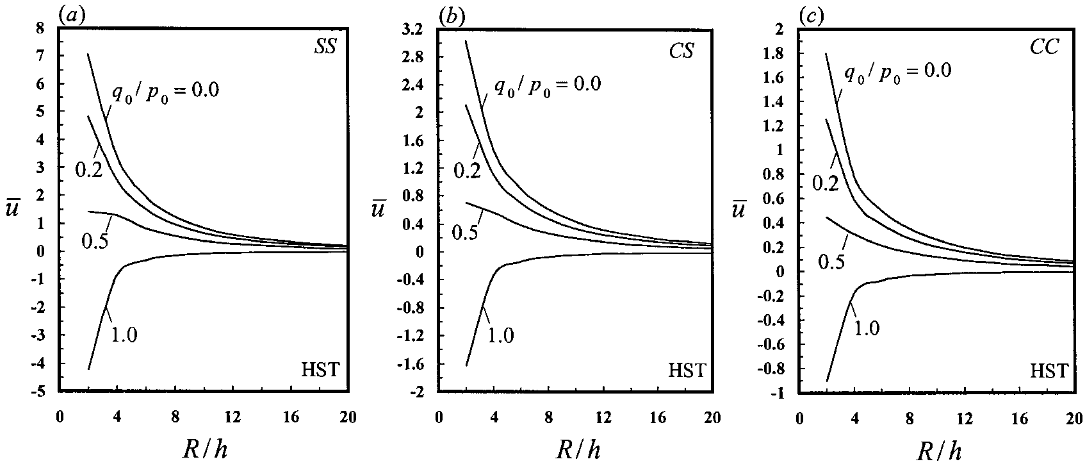

Figure 2. Maximum deflection *vs.* radius-to-thickness ratio of a (0°/90°/90°/0°) circular cylindrical shell subjected to: (a) simply supported edge conditions, (b) clamped-simply supported edge conditions, (c) clamped edge conditions.

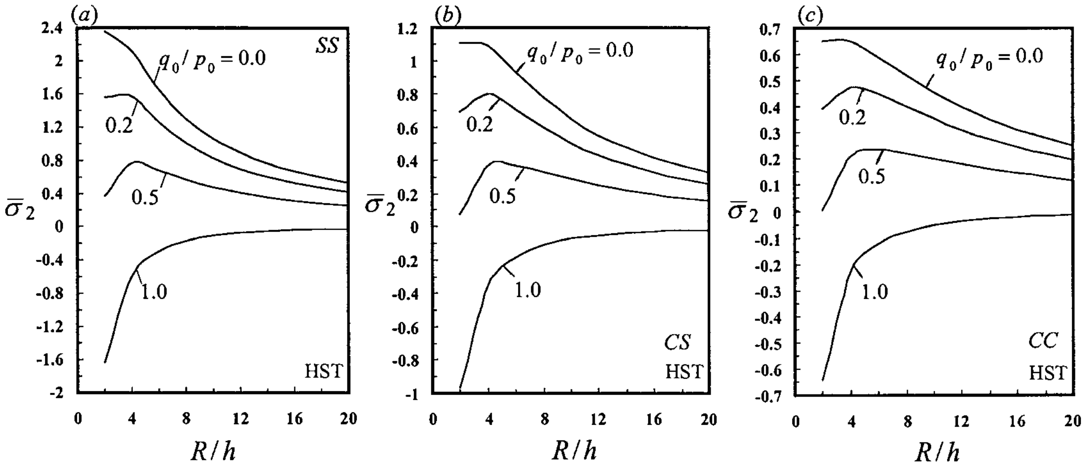

Figure 3. Circumferential stress *vs.* radius-to-thickness ratio of a (0°/90°/90°/0°) circular cylindrical shell subjected to: (a) simply supported edge conditions, (b) clamped-simply supported edge conditions, (c) clamped edge conditions.

7. Conclusions and discussion

The M–L mixed variational formula in conjunction with the Ritz method has been used to develop both the analytical and numerical solutions for bending analysis of a cross-ply axisymmetric shear deformable circular cylindrical shell. Several sets of numerical results for deflections and stresses are presented to show the effect of shear deformation, number of layers, boundary conditions, orthotropy ratio and loadings ratio on the static response of composite cylindrical shells. The numerical results presented in Tables 2–5 allow one to conclude the following:

(i) For thick shells the effect of transverse shear deformation must always be incorporated into the analysis, because CST underpredicts the deflections and overpredicts the stresses

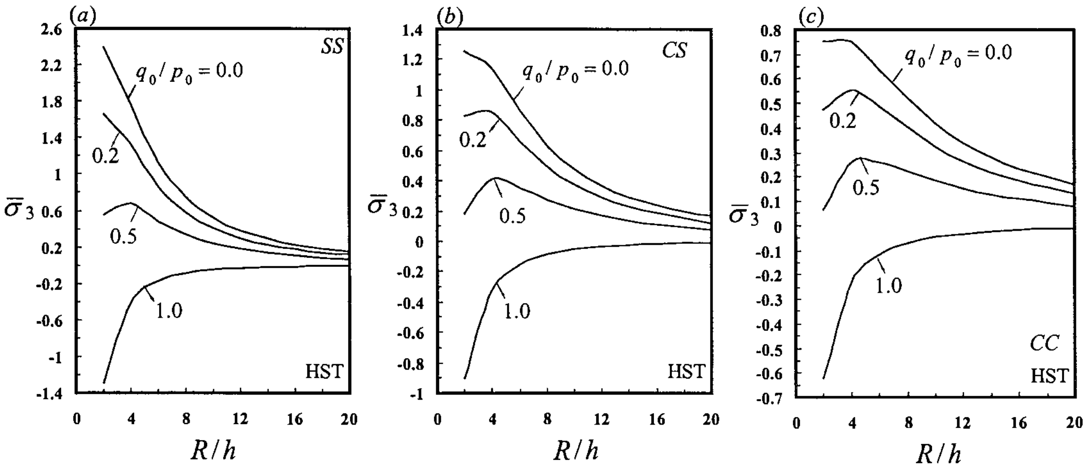

Figure 4. Axial stress *vs.* radius-to-thickness ratio of a (0°/90°/90°/0°) circular cylindrical shell subjected to: (a) simply supported edge conditions, (b) clamped-simply supported edge conditions, (c) clamped edge conditions.

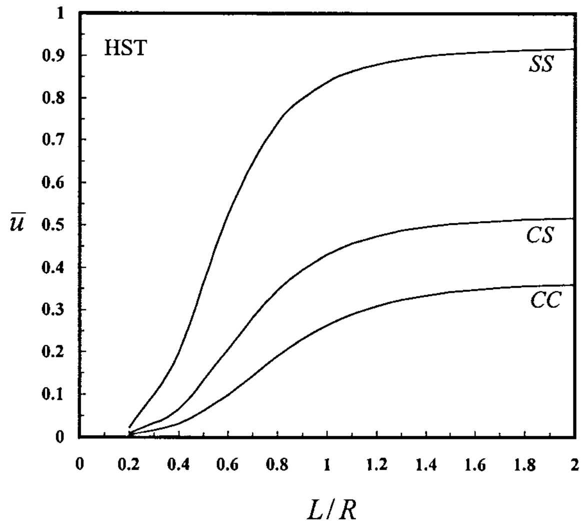

Figure 5. Effect of length-to-radius ratio (L/R) on $\bar{u}$ of a (0°/90°/0°/90°) circular cylindrical shell subjected to various boundary conditions.

when compared to FST and HST. An exception to this observation is provided by all boundary conditions for the case of $R/h = 2$ and by CS and CC boundary conditions for the case of $R/h = 4$ (see Table 3). For $R/h = 2$, the relative errors of $\bar{\sigma}_2$ predicted by CST differ by about 2%, 10% and 20% for shells subjected to SS, CS, and CC boundary conditions, respectively. Increasing the number of antisymmetric layers, for the same total thickness, will decrease the absolute relative errors CST-HST of deflections and stresses for all boundary conditions. In general, for thick and moderately thick shells with all boundary conditions, the symmetric cross-ply stacking sequence gives circumferential and axial stresses as predicted by CST with greater absolute relative errors than those of antisymmetric ones do. Moreover, the percentage errors CST-HST decrease (versus R/h) slowly in the case of axial stress when compared to the circumferential stress.

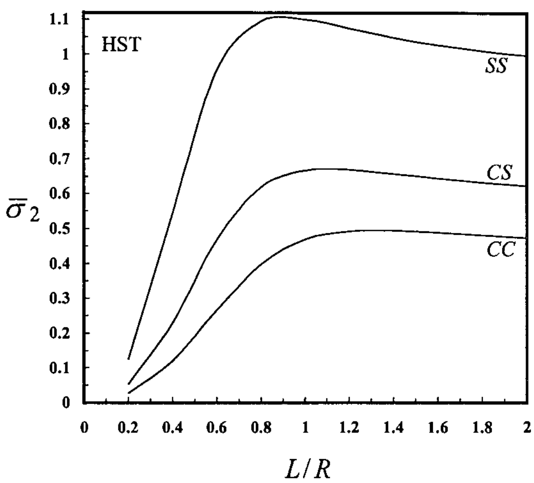

Figure 6. Effect of length-to-radius ratio (L/R) on $\bar{\sigma}_2$ of a (0°/90°/0°/90°) circular cylindrical shell subjected to various boundary conditions.

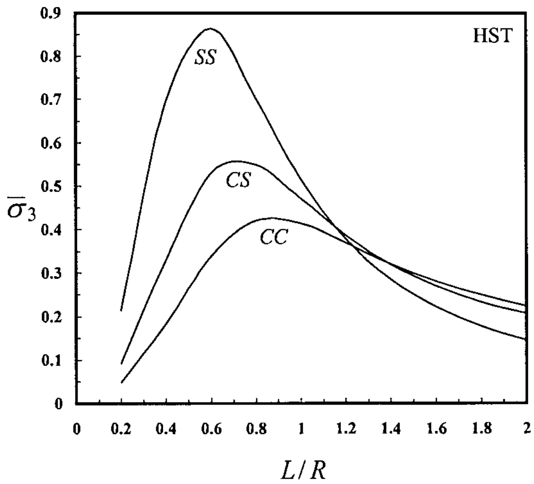

Figure 7. Effect of length-to-radius ratio (L/R) on $\bar{\sigma}_3$ of a (0°/90°/0°/90°) circular cylindrical shell subjected to various boundary conditions.

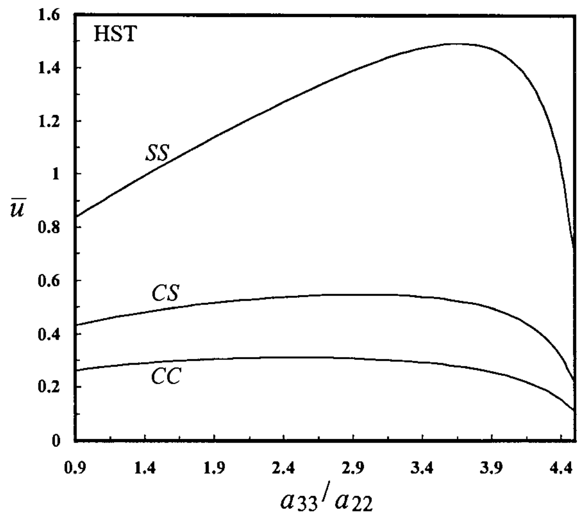

Figure 8 Effect of orthotropy ratio (a_{33}/a_{22}) on the center deflection ($\bar{u}$) of a (0°/90°/0°) circular cylindrical shell for various boundary conditions.

(ii) For thin shells the results predicted by the classical theory and the shear deformation theories are in excellent agreement. For moderately thick SS {CS and CC} shells, it is seen that the symmetric cross-ply stacking sequence gives deflection, for example, with a smaller {greater} relative error than those of antisymmetric ones do. In antisymmetric cross-ply arrangements, an increasing number of layers, for the same total thickness, will increase {decrease} the relative error. In this sense, the relative errors of deflection predicted by CST are 0·16%, 0·82%, and 2·68% for two-layer antisymmetric cross-ply cylindrical shells subjected to SS, CS, and CC boundary conditions, respectively.

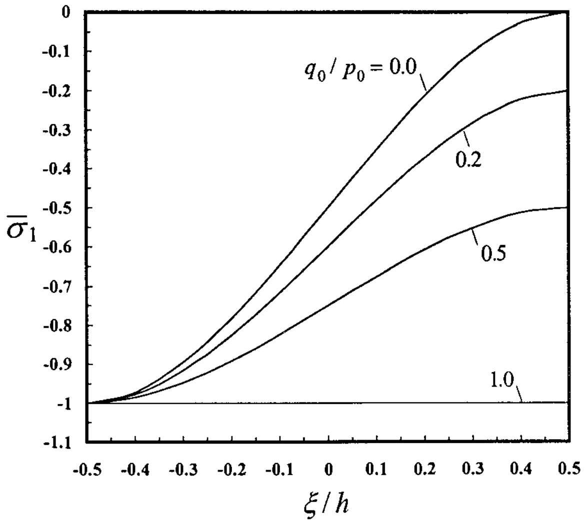

Figure 9 Plots of the radial stress ($\overline{\sigma}_1$) through the thickness of the shell.

(iii) The FST slightly overpredicts the deflections and stresses for shells subjected to various boundary conditions. The variation of the results obtained as per HST and FST exhibits a small difference, which increases when R/h decreases (see Tables 2–4). In fact, FST yields identical results with HST for thin shells and also for moderately thick shells under equal loads ($q_0/p_0 = 1$) and this irrespective of the considered boundary conditions (see Table 5).

Next, we will turn our attention to the effect of the boundary conditions, radius-to-thickness ratio, loadings ratio and length-to-radius ratio on the deflections and stresses of four-layer, symmetric and antisymmetric cross-ply cylindrical shells using HST only. Figures 2–7 are very revealing in this respect. In this sense the SS instance shows the highest sensitivity in the context of the considered edge conditions.

Figure 8 reveals that the variation of $\overline{u}$ is sensitive to the variation of the orthotropy ratio (a_{33}/a_{22}) and this depending on the considered boundary conditions. Figure 9 reveals also the sensitivity of $\overline{\sigma}_1$ to the variation of ξ/h parameter depending on the considered q_0/p_0 ratios. However, the case $q_0/p_0 = 1$ constitutes an exception, in the sense that the considered variation of ξ/h has no effect on the variation of $\overline{\sigma}_1$.

In general, the obtained results imply that the classical shell theory needs to be modified. It fails to predict accurately the static response when the cylindrical shells are thick or moderately thick. However, it provides reliable results compared to the shear deformation theories for thin shells. The first-order shell theory does not require the incorporation of shear correction factors and yields results that are very close to those of the higher-order theory. The analytical solutions presented here for cross-ply axisymmetric shear deformable laminated closed circular cylindrical shells subjected to arbitrary boundary conditions should serve as benchmark solutions for future comparisons.

Concerning the mathematical tool, namely the mixed variational approach, used in the determination of the state of stress and displacement of cylindrical shells for various edge conditions, it was shown to have great computational efficiency. It allows one to deal with the higher-order shell theory without using additional higher-order stress resultants and material stiffness coefficients. Moreover, when a representation of the displacement field consistent with the first-order shell theory is considered, its use precludes the incorporation of a shear correction factor. The mixed variational approach is also capable of providing solutions for the buckling and free-vibration problems of laminated cylindrical shells. The free-vibration problem has been presented in [22], while the buckling problem will be analyzed in another work.

Appendix A. Notation

The following symbols are given in this paper:

a, b	the inner and outer radii of the section of the shell
A_{ij}, B_{ij}, D_{ij}	extensional, coupling, and bending stiffnesses
a_{ij}	compliance constants (strain coefficients)
E_i	Young's moduli
ξ	thickness coordinate
ξ_0, ξ_N	the inner ($\xi_0 = -h/2$) and outer ($\xi_N = +h/2$) surfaces of the shell
ξ_{k-1}, ξ_k	the inner and outer ξ-coordinates of the kth lamina
φ	the rotation at $\xi = 0$ of normal to the mid-surface
G_{ij}	shear moduli
h, L	total thickness and length of the shell
N	number of layers of the shell
N_i, M_i, Q	normal stress, moment, and shear stress resultants
ν_{ij}	Poisson's ratios
R	radius of the mid-surface of the shell
r, θ, z	radial, circumferential, and axial cylindrical coordinates
p, q	internal and external loads applied on lateral surface of the shell
u, w	displacements of a point on the mid-surface
$u_i, \sigma_{ij}, \varepsilon_{ij}$	displacement, stress, and strain components
U_m, W_m, Φ_m	amplitudes of u, w, φ associated with mth axial component
u_r, u_z	radial and axial displacements

Appendix B.

The elements $C_{ij} = C_{ji}$ of matrix $[C]$ are given by:

$$C_{11} = \frac{A_{22}^*}{R^2}\Psi_1 + \mu_m^2\left(\alpha + \frac{3h^2}{20}\gamma\right)\left[\frac{2B_{23}^*}{R}\Psi_4 + D_{33}^*\Psi_3\mu_m^2\left(\alpha + \frac{3h^2}{20}\gamma\right)\right]$$

$$+A_{55}^*\Psi_2\mu_m^2\left(1 + \alpha + \frac{3h^2}{20}\gamma\right)^2,$$

$$C_{12} = \frac{A_{23}^*}{R}\Psi_4\mu_m + B_{33}^*\Psi_3\mu_m^3\left(\alpha + \frac{3h^2}{20}\gamma\right),$$

$$C_{13} = \mu_m \left(\beta + \frac{3h^2}{20}\gamma\right)\left[A^*_{55}\Psi_2\left(1+\alpha+\frac{3h^2}{20}\gamma\right) + \frac{B^*_{23}}{R}\Psi_4 + D^*_{33}\Psi_3\mu_m^2\left(\alpha+\frac{3h^2}{20}\gamma\right)\right],$$

$$C_{22} = A^*_{33}\Psi_3\mu_m^2, \quad C_{23} = B^*_{33}\Psi_3\mu_m^2\left(\beta+\frac{3h^2}{20}\gamma\right), \quad C_{33}=\left(\beta+\frac{3h^2}{20}\gamma\right)^2\left[A^*_{55}\Psi_2 + D^*_{33}\Psi_3\mu_m^2\right],$$

where

$$\begin{bmatrix} A^*_{22} & A^*_{23} & 0 & B^*_{22} & B^*_{23} \\ & A^*_{33} & 0 & B^*_{32} & B^*_{33} \\ & & A^*_{55} & 0 & 0 \\ & & & D^*_{22} & D^*_{23} \\ \text{symm.} & & & & D^*_{33} \end{bmatrix} = \begin{bmatrix} A_{22} & A_{23} & 0 & B_{22} & B_{23} \\ & A_{33} & 0 & B_{23} & B_{33} \\ & & A_{55} & 0 & 0 \\ & & & D_{22} & D_{23} \\ \text{symm.} & & & & D_{33} \end{bmatrix}^{-1},$$

and

$$\Psi_1 = \int_0^L \left[\chi(\mu_m z)\right]^2 \, \mathrm{d}z, \quad \Psi_2 = \int_0^L \left[\chi'(\mu_m z)\right]^2 \mathrm{d}z,$$

$$\Psi_3 = \int_0^L \left[\chi''(\mu_m z)\right]^2 \, \mathrm{d}z, \quad \Psi_4 = \int_0^L \chi(\mu_m z)\chi''(\mu_m z) \, \mathrm{d}z.$$

Also the elements of the force vector are given by

$$\begin{aligned} F_1^m = {} & \left[p_0 - q_0 - \frac{h}{2R}(p_0+q_0)\right]\Psi_5 \\ & - \left[\frac{A^*_{22}}{R}\Psi_5 + B^*_{23}\Psi_6\mu_m^2\left(\alpha+\frac{3h^2}{20}\gamma\right)\right]\left(A_{12}^{(-1)}p_0 + A_{12}^{(+1)}q_0\right) \\ & - \left[\frac{A^*_{23}}{R}\Psi_5 + B^*_{33}\Psi_6\mu_m^2\left(\alpha+\frac{3h^2}{20}\gamma\right)\right]\left(A_{13}^{(-1)}p_0 + A_{13}^{(+1)}q_0\right) \\ & - \left[\frac{B^*_{22}}{R}\Psi_5 + D^*_{23}\Psi_6\mu_m^2\left(\alpha+\frac{3h^2}{20}\gamma\right)\right]\left(B_{12}^{(-1)}p_0 + B_{12}^{(+1)}q_0\right) \\ & - \left[\frac{B^*_{23}}{R}\Psi_5 + D^*_{33}\Psi_6\mu_m^2\left(\alpha+\frac{3h^2}{20}\gamma\right)\right]\left(B_{13}^{(-1)}p_0 + B_{13}^{(+1)}q_0\right), \\ F_2^m = {} & -\Psi_6\mu_m\left[A^*_{23}\left(A_{12}^{(-1)}p_0 + A_{12}^{(+1)}q_0\right) + A^*_{33}\left(A_{13}^{(-1)}p_0 + A_{13}^{(+1)}q_0\right)\right. \\ & \left. + B^*_{32}\left(B_{12}^{(-1)}p_0 + B_{12}^{(+1)}q_0\right) + B^*_{33}\left(B_{13}^{(-1)}p_0 + B_{13}^{(+1)}q_0\right)\right], \\ F_3^m = {} & -\Psi_6\mu_m\left(\beta+\frac{3h^2}{20}\gamma\right)\left[B^*_{23}\left(A_{12}^{(-1)}p_0 + A_{12}^{(+1)}q_0\right) + B^*_{33}\left(A_{13}^{(-1)}p_0 + A_{13}^{(+1)}q_0\right)\right. \\ & \left. + D^*_{23}\left(B_{12}^{(-1)}p_0 + B_{12}^{(+1)}q_0\right) + D^*_{33}\left(B_{13}^{(-1)}p_0 + B_{13}^{(+1)}q_0\right)\right], \end{aligned}$$

where

$$\Psi_5 = \int_0^L \chi(\mu_m z) \sin \frac{\pi z}{L}\, \mathrm{d}z, \quad \Psi_6 = \int_0^L \chi''(\mu_m z) \sin \frac{\pi z}{L}\, \mathrm{d}z.$$

References

1. A. Zingoni, *Shell Structures in Civil and Mechanical Engineering*. New York: Thomas Telford (1997) 349 pp.
2. A. E. H. Love, On the small free vibrations and deformations of a thin elastic shell. *Phil. Trans. R. Soc. Lond. A*179 (1888) 491–546.
3. E. Reissner, Stress-strain relations in the theory of thin elastic shells. *J. Math. Phys.* 31 (1952) 109–119.
4. P. M. Naghdi, On the theory of thin elastic shells. *Q. Appl. Math.* 14 (1957) 369–380.
5. S. P. Timoshenko and J. M. Gere, *Theory of Elastic Stability*. New York: McGraw-Hill (1961) 540 pp.
6. J. N. Reddy, *Energy and Variational Principles in Applied Mechanics*. New York: Wiley (1984) 560 pp.
7. J. A. Zukas, Effect of transverse normal and shear strains in orthotropic shells. *AIAA J.* 12 (1974) 1753–1755.
8. J. M. Whitney and C. T. Sun, A refined theory for laminated anisotropic cylindrical shells. *J. Appl. Mech.* 41 (1974) 471–476.
9. C. T. Sun and J. M. Whitney, Axisymmetric vibrations of laminated composite cylindrical shells. *J. Acoust. Soc. Am.* 55 (1974) 1238–1246.
10. L. Librescu, *Elastostatics and Kinetics of Anisotropic and Heterogeneous Shell-Type Structures*. Leyden: Noordhoff (1975) 593 pp.
11. M. Brull and L. Librescu, Strain measures and compatibility equations in the linear high-order shell theories. *Q. Appl. Math.* 40 (1982) 15–25.
12. G. Yamada, T. Irie and M. Tsushima, Vibration and stability of orthotropic circular cylindrical shells subjected to axial load. *J. Acoust. Soc. Am.* 75 (1984) 842–848.
13. J. N. Reddy, Exact solutions of moderately thick laminated shells. *J. Eng. Mech.* 110 (1984) 794–809.
14. J. N. Reddy and C. F. Liu, A higher-order shear deformation theory of laminated elastic shells. *Int. J. Eng. Sci.* 23 (1985) 319–330.
15. L. Librescu, Refined geometrically nonlinear theories of anisotropic laminated shells. *Q. Appl. Math.* 45 (1987) 1–22.
16. A. A. Khdeir, J. N. Reddy and D. Fredrick, A study of bending, vibration and buckling of cross-ply circular cylindrical shells with various shell theories. *Int. J. Eng. Sci.* 27 (1989) 1337–1351.
17. J. N. Reddy and E. J. Barbero, General two-dimensional theory of laminated cylindrical shells. *AIAA J.* 28 (1990) 544–553.
18. V. Birman, Exact solution of axisymmetric problems of laminated cylindrical shells with arbitrary boundary conditions–higher-order theory. *Mech. Res. Comm.* 19 (1992) 219–225.
19. F. Fraternali and J. N. Reddy, A penalty model for the analysis of laminated composite shells. *Int. J. Solids Struct.* 30 (1993) 3337–3355.
20. L. Librescu and W. Lin, Two models of shear deformable laminated plates and shells and their use in prediction of global response behavior. *Eur. J. Mech. A/Solids* 15 (1996) 1095–1120.
21. E. Carrera, A Reissner's mixed variational theorem applied to vibration analysis of multilayered shell. *J. Appl. Mech.* 66 (1999) 69–78.
22. A. M. Zenkour, Vibration of axisymmetric shear deformable cross-ply laminated cylindrical shells – a variational approach. *Int. J. Eng. Sci.* 36 (1998) 219–231.
23. A. M. Zenkour, Maupertuis-Lagrange mixed variational formula for laminated composite structures with a refined higher-order beam theory. *Int. J. Non-Lin. Mech.* 32 (1997) 989–1001.
24. A. M. Zenkour, Natural vibration analysis of symmetrical cross-ply laminated plates using a mixed variational formulation. *Eur. J. Mech. A/Solids* 19 (2000) 469–485.
25. M. E. Fares and A. M. Zenkour, Mixed variational formula for the thermal bending of laminated plates. *J. Thermal Stresses* 22 (1999) 347–365.
26. M. E. Fares, A. M. Zenkour and M. Kh. El-Marghany, Non-linear thermal effects on the bending response of cross-ply laminated plates using refined first-order theory. *Compos. Struct.* 49 (2000) 257–267.
27. A. M. Zenkour and Y. G. Youssif, Free vibration analysis of symmetric cross-ply laminated elastic plates. *Mech. Res. Comm.* 27 (2000) 165–172.

28. A. M. Zenkour and M. E. Fares, Thermal bending analysis of composite laminated cylindrical shells using a refined first-order theory. *J. Thermal Stresses* 23 (2000) 505–526.
29. M. E. Fares, M. N. M. Allam and A. M. Zenkour, Hamilton's mixed variational formula for dynamical problems of anisotropic elastic bodies. *Solid Mech. Arch.* 14 (1989) 103–114.
30. A. M. Zenkour, Buckling and free vibration of elastic plates using simple and mixed shear deformation theories. *Acta Mech.* (2001) in press.
31. S. G. Lekhnitskii, *Theory of Elasticity of an Anisotropic Body*. Moscow: Mir (1981) 430 pp.
32. J. N. Reddy, *Theory and Analysis of Elastic Plates*. Philadelphia: Taylor & Francis (1999) 576 pp.